

# Finite Element Formulation of Radioisotope Diffusion in Metal Grain Textures

FERNANDO G. BASOMBRÍO

*Centro Atómico Bariloche, Comisión Nacional de Energía Atómica,  
8400 S.C. de Bariloche (R.N.), Argentina*

Received October 22, 1982; revised June 21, 1983

The problem of grain boundary diffusion of radioisotopes is analysed by the finite element method for a plane semiinfinite situation. Mathematically this problem consists of solving the time-dependent linear diffusion equation with a fixed Dirichlet condition at the finite rectilinear boundary. But peculiarities arise because of the existence of a thin straight region (the grain boundary) of about  $10^{-8}$  cm width separating two grains, whose conductivity is five orders of magnitude greater than that of the metal grains. Reasonable solutions were obtained by using quadrilateral Lagrange elements for the grains on the central finite region and one-dimensional linear elements for the grain boundary. The main purpose of the paper is to establish the underlying ideas for a natural finite element formulation of this kind of problem, based on a variational approach.

## 1. GENERALITIES

We wish to present some simple ideas related to the variational formulation of the problem of radioisotope penetration in metals. See, for example, [1, 2] and references quoted here. Such radioisotope diffusion is governed by the same laws as a linear time-dependent heat conduction problem, with concentrations instead of temperatures.

Suppose a semi-infinite metal extended in the semiplane  $x \geq 0$  (Fig. 1). We distinguish two metal grains  $\alpha$  and  $\beta$  with different diffusivities  $K_\alpha$  and  $K_\beta$ , respectively, for  $y < -a$  and  $y > +a$ . The region  $x \geq 0$ , and  $-a \leq y \leq +a$  is designated as the "grain boundary" or "interface boundary," and characterized by the diffusivity  $K_i$ . Under the constant concentration source hypothesis [1] the formulation of this idealized model of grain boundary diffusion, consists of assuming a constant Dirichlet condition  $c = 100$  ( $c =$  concentration of radioisotope) at  $x = 0$  and then adopting the usual Fourier law in the heterogeneous material shown in Fig. 1. A Neumann-type condition is imposed at infinity for  $x \geq 0$ .

For computational purposes it suffices to consider a finite rectangular region instead of the semi-infinite one. But this is just the case for diffusion experiments where the specimens have rectangular form and dimensions of the order indicated in Fig. 1. Furthermore, it is assumed that the problem is independent of the coordinate  $z$ .

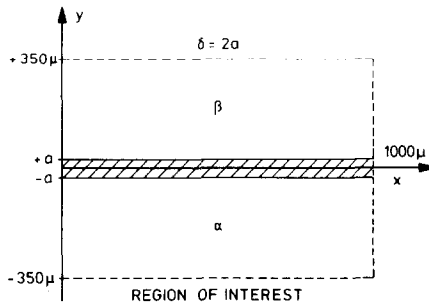


FIG. 1. Schematic presentation of the problem's geometry.

Up to the moment, this is a classical time-dependent and heterogeneous two-dimensional problem. Nevertheless difficulties arise when considering the extremely small value of  $a$  ( $\approx 10^{-4}\mu$ ;  $\mu = \text{micron}$ ) in comparison with the typical dimension of the specimen; and the high value of  $K_i$  ( $\approx 10^4 \mu^2/\text{seg}$ ) also in relation to the values  $K_\alpha \approx -1.7 \times 10^{-1} \mu^2/\text{seg}$  and  $K_\beta = -5 \times 10^{-1} \mu^2/\text{seg}$ . The differences are of seven and five orders of magnitude, respectively.

Mathematically the problem could be stated as follows: the limit of the classical formulation when

$$\begin{aligned} a &\rightarrow 0 \\ K_i &\rightarrow -\infty \end{aligned} \quad (1)$$

but

$$aK_i \rightarrow \text{const} \neq 0 \quad (2)$$

The latter is the same as saying that the one-dimensional conductivity of the grain boundary  $y = 0$  subsists, making the problem of interest.

Analytical solutions for the symmetric case ( $K_\alpha = K_\beta$ ) have been known for a long time [1] but they are not easy to handle. The possibility of having numerical models available is then of special interest.

## 2. SOME MATHEMATICAL ASPECTS

The variational formulation of the classical problem for the source-free case is

$$\left( \frac{\partial c}{\partial t}, v \right) + a(c, v) = 0 \quad (3)$$

for every  $v$  belonging to an appropriate functional space. The following notation is used:

$$\begin{aligned}
 (\theta, \psi) &\equiv \int_{-\infty}^{\infty} \int_0^{\infty} \theta \psi \, dx \, dy \\
 a(\theta, \psi) &= - \int_{-\infty}^{\infty} \int_0^{\infty} K \left( \frac{\partial \theta}{\partial x} \frac{\partial \psi}{\partial x} + \frac{\partial \theta}{\partial y} \frac{\partial \psi}{\partial y} \right) dx \, dy
 \end{aligned} \tag{4}$$

Inspired by [1] we now develop the solution  $c(x, y, t)$  in power series of  $y$  for  $-a \leq y \leq a$  and proceed to the integration.

Admitting the continuity of the solution and a reasonable regularity of it for  $y \neq \pm a$ , we finally obtain

$$\begin{aligned}
 a(c, v) &\equiv - \int_{-\infty}^{-a} \int_0^{\infty} K_{\alpha} \left( \frac{\partial c}{\partial x} \frac{\partial v}{\partial x} + \frac{\partial c}{\partial y} \frac{\partial v}{\partial y} \right) dx \, dy \\
 &\quad - \int_a^{+\infty} \int_0^{\infty} K_{\beta} \left( \frac{\partial c}{\partial x} \frac{\partial v}{\partial x} + \frac{\partial c}{\partial y} \frac{\partial v}{\partial y} \right) dx \, dy \\
 &\quad - \int_0^{\infty} 2aK_t \frac{\partial c}{\partial x} \frac{\partial v}{\partial x} dx \\
 &\quad + \mathcal{O}(a^2 K_t) + \mathcal{O}(a^3)
 \end{aligned} \tag{5}$$

and

$$\begin{aligned}
 \left( \frac{\partial c}{\partial t}, v \right) &\equiv \int_{-\infty}^{-a} \int_0^{\infty} \frac{\partial c}{\partial t} v \, dx \, dy + \int_a^{\infty} \int_0^{\infty} \frac{\partial c}{\partial t} v \, dx \, dy \\
 &\quad + 2a \int_0^{\infty} \frac{\partial c}{\partial t} v \, dx + \mathcal{O}(a^2)
 \end{aligned} \tag{6}$$

For the actual problem, the variational formulation is simply obtained by the application of the limiting process (1) and (2) to expressions (5) and (6) to be used in (3). In this way

$$\begin{aligned}
 a(c, v) &\equiv - \int_{-\infty}^{\infty} \int_0^{\infty} K \left( \frac{\partial c}{\partial x} \frac{\partial v}{\partial x} + \frac{\partial c}{\partial y} \frac{\partial v}{\partial y} \right) dx \, dy \\
 &\quad - \int_0^{\infty} 2aK_t \frac{\partial c}{\partial x} \frac{\partial v}{\partial x} dx
 \end{aligned} \tag{7}$$

$$\left( \frac{\partial c}{\partial t}, v \right) = \int_{-\infty}^{\infty} \int_0^{\infty} \frac{\partial c}{\partial t} v \, dx \, dy + 2a \int_0^{\infty} \frac{\partial c}{\partial t} v \, dx$$

It is noted that formally the last term of the second expression should be dropped.

We have kept it because even with  $a$  very small, in the first instants of the phenomenon  $\partial c/\partial t$  takes high values so that this term should, in principle, be conserved. Nevertheless, the numerical experiences have shown that its contribution is not significant, at least for the particular cases solved.

For the expected solutions, that is, those continuous and sufficiently regular for  $y \neq 0$ , the variational formulation (3), (7) yields (through the classical procedure) the set of well-known equations [2]:

$$\begin{aligned} \frac{\partial c}{\partial t} + K\nabla^2 c &= 0 & \text{for } y \neq 0 \quad (K = K_\alpha, K_\beta) \\ \rho \frac{\partial c}{\partial t} + \sigma \frac{\partial^2 c}{\partial x^2} &= \phi(x) & \text{for } y = 0 \end{aligned} \quad (8)$$

where  $\nabla$  stands for the gradient operator,  $\rho = 2a$ ,  $\sigma = 2aK_i$  and

$$\phi(x) = K_\alpha \left. \frac{\partial c}{\partial y} \right|_{y=0^-} - K_\beta \left. \frac{\partial c}{\partial y} \right|_{y=0^+} \quad (9)$$

Whipple's equations [1] are immediately recovered for the symmetric case.

We conclude this section by noting that the variational formulation (3), (7) should be defined for appropriate functional spaces of functions with finite trace over  $y = 0$ .

### 3. FINITE ELEMENT APPROXIMATION

This is a direct consequence of the discretized interpretation of (3) and (7). The two-dimensional terms of (7) require plane elements and the single integral ones, the introduction of one-dimensional elements at  $y = 0$ . For the former we adopted the usual quadrilateral isoparametric Lagrange elements with bilinear interpolating functions, and for the latter, linear one-dimensional elements. The mesh is shown in Fig. 2. It was automatically generated with the program KUBIK [5].

In the first calculations the region was covered to infinity by infinite elements with decay  $r^{-p}$ , where  $r$  is roughly the distance (radius) to the central part. Later it was observed that they produce no significant changes in the solution, so they were finally abandoned.

The computer program contains sparse matrix subroutines [3], uses the Crank-Nicolson time discretization scheme, and the incremental algorithm for the time steps [4].

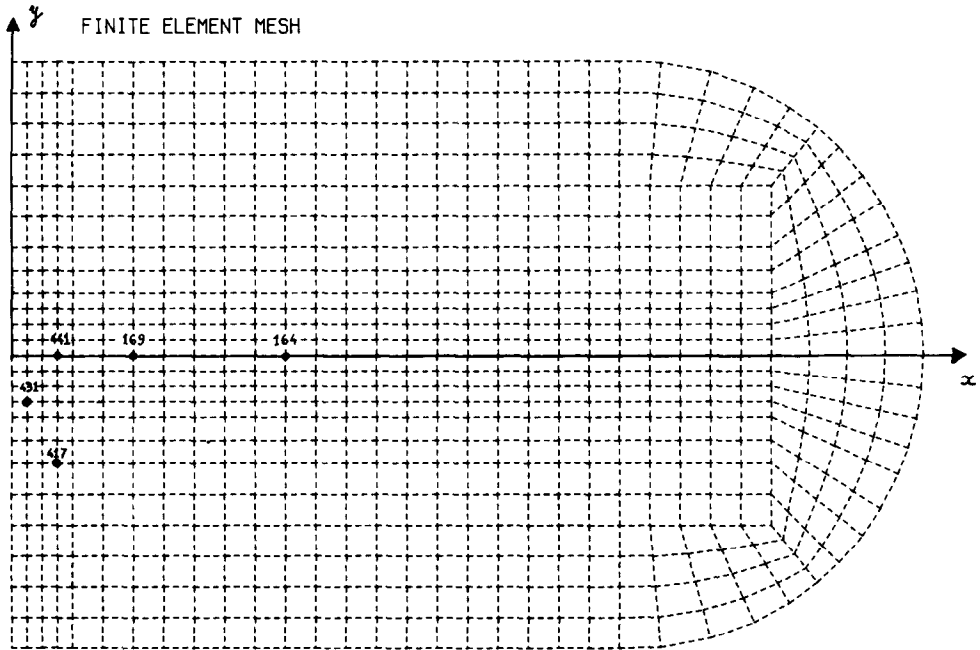


FIG. 2. Finite element mesh. The one-dimensional elements stay on the line  $y=0$ . Points where a comparison was made with the exact solution are indicated.

TABLE I  
Comparison<sup>a</sup> Between the Finite Element Solution (FEM) and the Exact Solution (Whipple, 1954) for the symmetric Problem at the Points Indicated in Fig. 2.

		Node	164	169	417	431	441
		Time					
5 h	FEM	—	6.520	38.06	78.34	48.47	
	REL.	—	0.917	0.991	1.000	0.997	
10 h	FEM	—	16.72	54.11	84.75	60.26	
	REL.	—	0.983	0.998	1.000	0.999	
15 h	FEM	0.997	24.65	62.08	87.55	66.29	
	REL.	0.897	0.994	0.999	1.000	1.000	
20 h	FEM	2.258	30.73	67.00	89.20	70.12	
	REL.	0.936	0.997	1.000	1.000	1.000	

<sup>a</sup> The comparison is represented by the quotient (REL.) between the FEM solution and the exact one when the value of the solution is greater than 1.0.

## 4. NUMERICAL RESULTS

Two examples were solved. The first one is a comparison with the exact solution of Whipple [1] for  $K_\alpha = K_\beta = -0.1 \mu^2/\text{seg}$ ,  $K_i = -10^4 \mu^2/\text{seg}$ , and  $a = 2.5 \times 10^{-4} \mu$ . The results (see Table I) show a very satisfactory agreement between the FEM solutions and the exact one except, of course, for low values of the solution (initial

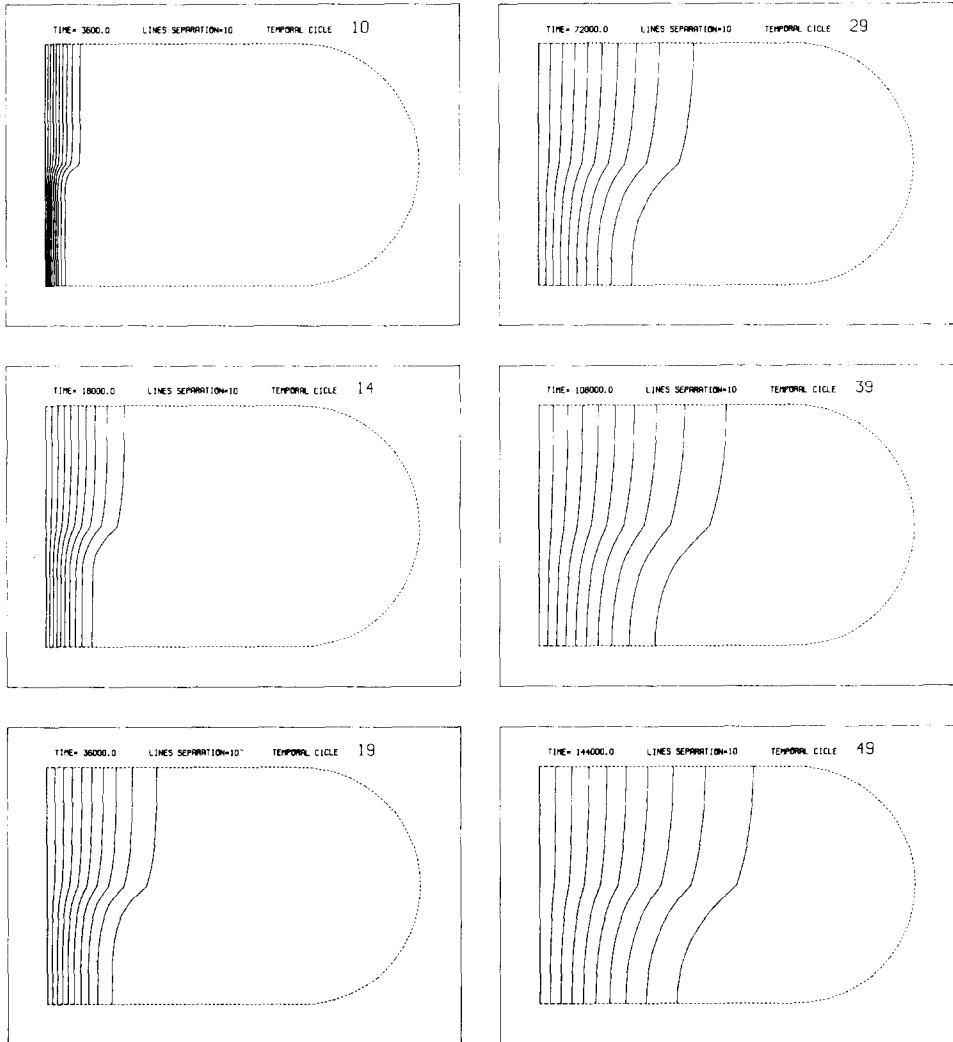


FIG. 3. Lines of equal concentration for different times: 1 h, 5 h, 10 h, 20 h, 30 h, 40 h. Line separation is 10.

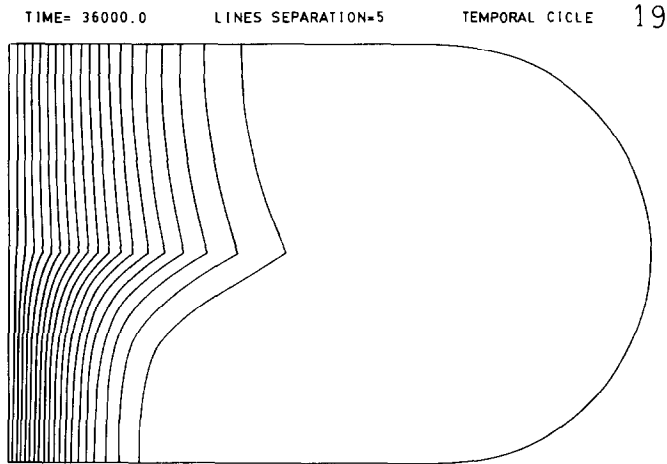


FIG. 4. Similar problem, showing the "cusp effect," for a value of  $K_i$  an order of magnitude greater than for the preceding case. Time: 10 h.

times or remote spatial points). For these values, as usual, the relative numerical errors are much greater than for the higher values.

The second case is one of physical interest ( $K_\alpha = -1.7 \times 10^{-1} \mu^2/\text{seg}$ ,  $K_\beta = -5.0 \times 10^{-1} \mu^2/\text{seg}$ ,  $K_i = -10^4 \mu^2/\text{seg}$  and  $a = 2.5 \times 10^{-4} \mu$ ). The results, shown in Fig. 3, do not make at all evident the importance of the interfacial region ("cusp effect"). To exhibit this effect more clearly, an additional calculation was performed with the same data, but now with the boundary grain conductivity raised to the (perhaps unphysical) value  $K_i = -1.3 \times 10^5 \mu^2/\text{seg}$ , an order of magnitude greater than the preceding case (see Fig. 4). The plotted outputs show a quite reasonable behaviour for the lines of equal concentration at different times. The cusp effect is very important for the first case (Whipple's solution) but the equal concentration lines are not included in the paper.

## 5. DISCUSSION

A variational formulation has been described for the problem of a highly conducting one-dimensional channel immersed in a less conducting two-dimensional medium, leading in a natural way to a discretization using one-dimensional and two-dimensional elements, respectively.

The underlying idea (and the variational formulation (3), (7)) can immediately be extended to linear and nonlinear problems of greater dimension (conducting lines or surfaces in three-dimensional media, for example). Also, no conceptual difficulty arises if the conducting channels form general irregular curved meshes. Nevertheless

for such peculiar cases, the usual formulation through differential equations becomes essentially obscure.

#### ACKNOWLEDGMENTS

The author remains especially grateful to Dra. F. Dymont (Centro Atómico Constituyentes–Comisión Nacional de Energía Atómica–Argentina) for formulating the problem and the stimulus given for solving it; to Lic. E. Forlerer (CAC–CNEA) for her valuable and enthusiastic cooperation; to Dr. S. Pissanetzky (Centro Atómico Bariloche–CNEA) for facilitating us the sparse matrix subroutines package and the KUBIK program; finally to N. Callwood (CAB–CNEA) for elaborating an efficient subroutine to calculate the exact solution of Whipple.

#### REFERENCES

1. R. T. P. WHIPPLE, *Philos. Mag.*, **45** (1954), 1225–1236.
2. J. E. RUZZANTE AND F. DYMENT, *Com. Nac. Energ. Atómica. Argentina CNEA-IN 5/146*, 1974. [in Spanish]
3. S. PISSANETZKY, *Centro de Cómputos. Centr. Atom. Bariloche. CNEA*, 1980.
4. S. PISSANETZKY AND F. G. BASOMBRÍO, *Numer. Math.* **38** (1981), 31–37.
5. S. PISSANETZKY, *Intern. J. Num. Methods Engng* **17** (1981), 255–269.